Case Studies in Thermal Engineering 36 (2022) 102202

Contents lists available at ScienceDirect

Case Studies in Thermal Engineering

journal homepage: www.elsevier.com/locate/csite

A coupled hybrid numerical study of tunnel longitudinal ventilation under fire conditions

Diego Álvarez-Coedo [a], Pablo Ayala [a,*], Alexis Cantizano [a], Wojciech Węgrzyński [b]

[a] Institute for Research in Technology, ICAI, Comillas Pontifical University, c/ Sta. Cruz de Marcenado, 26, 28015, Madrid, Spain
[b] ITB: Instytut Techniki Budowlanej, ul. Filtrowa 1, 00-611, Warszawa, Poland

ARTICLE INFO

Keywords:
CFD
Coupled hybrid modelling
Tunnel ventilation
Tunnel fires
FDS
Full-scale tests

ABSTRACT

This paper presents the validation of a coupled hybrid (1D/3D-CFD) modelling methodology, using FDS version 6.7.5, for the first time, with full-scale fire tests. Real fire conditions of the Runehamar tests with maximum heat release rates of 6 MW, 66 MW, and 119 MW are compared by assessing temperature profiles, centreline velocity, backlayering lengths, and maximum temperatures at different locations both upstream and downstream from the fire source. An expression to evaluate the length of the 3D domain where the fire is located is successfully assessed. Also, a pressure boundary condition at one of the portals is suggested to predict more precisely the inner flow conditions. The temperature profiles are accurately predicted with time-averaged differences lower than 20% beyond 40 m downstream from the fire source in the three tests. Furthermore, with the coupled hybrid approach, the backlayering length is estimated accurately with the fire of 66 MW and underestimated in the 6 MW and 119 MW fires, i.e. a maximum difference lower than 4% of the total tunnel length. The validated proposed methodology allows accurate predictions of temperature for tunnel fires and reduces the computational cost between 27% and 75% with respect to a full-CFD numerical model.

1. Introduction

Fire in tunnels can become catastrophic due to its narrow and long structures, hindering evacuation or emergency operations and causing relevant economic and social losses [1]. Many different topics related to tunnel ventilation, internal temperature fields, and smoke hazards are being researched, such as the influence of fire locations [2–4], the impact of wind [5], the number of vehicles trapped [6,7], the maximum gas temperature rise beneath the ceiling [8,9], or even the optimal distance between jet fans, [10].

Nowadays, the use of Computational Fluid Dynamics (CFD) simulations to assess tunnel ventilation systems under diverse internal and external conditions is broadly extended [11,12]. Nonetheless, the analysis of their critical performance factors is always computationally expensive, mainly due to tunnel dimensions and the number of simulations required for a wide range of possible fire scenarios. In such a context, "coupled hybrid" modelling [13], which refers to using a single numerical tool with multiple sub-models of different complexities, may become a powerful and promising solution as concluded in Ref. [13]. Here, a tunnel modelled by a combination of 3D and 1D regions is denoted as a coupled hybrid model [14–16], despite other fields using terms like integrated, multi-scale, two-scale, 3D-1D, etc. Thus, in those tunnel regions with complex flow patterns or relevant temperature gradients, such as jet-fans, portals, or in the near-field of a fire, complex 3D regions are defined and simulated with field models, in this case a CFD

* Corresponding author. Escuela Técnica Superior de Ingeniería (ICAI), c/ Alberto Aguilera, 25, 28015, Madrid. Spain.
E-mail address: pablo.ayala@iit.comillas.edu (P. Ayala).

https://doi.org/10.1016/j.csite.2022.102202
Received 14 December 2021; Received in revised form 30 May 2022; Accepted 11 June 2022
Available online 14 June 2022

Nomenclature

C_p	Specific heat capacity of air (kJ/(kg K))
D^*	Characteristic diameter of the plume (m)
Fr	Froude number
g	Gravity acceleration (m/s^2)
$\overline{H}$	Tunnel hydraulic diameter (m)
L	Tunnel length (m)
L_{crit}	Central 3D-CFD critical length (m)
L^*	Dimensionless critical length (m)
$\dot{Q}$	Heat release rate (kW)
Q^*	Dimensionless heat release rate
R	Spatial resolution
T_{avg}	Average Temperature (K)
T_c	Ceiling Temperature (K)
T_f	Floor Temperature (K)
T_∞	Air Temperature (K)
U	Longitudinal velocity (m/s)
Δ	Cell size (m)
ρ_∞	Air Density (kg/m^3)

software. For the rest of the tunnel, where the flow is primarily unidirectional, simpler 1D models are used, generally based on empirical correlations. The coupling of both sub-models is key for achieving an efficient and fast numerical model.

This coupled hybrid approach was originally presented in Refs. [17,18] to assess the Dartford tunnel's longitudinal ventilation system (without fire) using ANSYS Fluent by comparing the results with full-scale tests. Cold flow experimental tests in the same tunnel were also validated by a coupled hybrid approach using FDS 6.1.1. (Fire Dynamics Simulator) in Ref. [19], in which the background velocity was simulated by introducing two unreal slot fans at the tunnel entrance. Numerical fire scenarios, using a coupled hybrid approach with ANSYS Fluent, were analyzed in Refs. [14,17] to study the backlayering length with transient flows. The computational cost was reduced 40 times in relation to a complete CFD simulation. The same tunnel was modelled with FDS 6.0, with a fire load in the centre of the tunnel and including the ventilation system in the 1D domain [20]. A computational cost reduction of 99% was achieved. Nevertheless, this study also pointed out numerical oscillations in the mass flow and in the temperatures, which required careful investigation as it was discussed in Refs. [21,22].

Here, this paper is focused on experimental validation of coupled hybrid modelling in tunnel fire scenarios using open-source software (FDS), which was identified in Ref. [13] as so far insufficient and required for the future use of this tool by the industry. In fact, all the previously mentioned studies with coupled hybrid models were only focused on the numerical approach, and they were not compared with fire experimental data. As it was concluded in Ref. [23], the numerical prediction of the scale experiments is more precise and simpler. Full-scale simulations are challenging mainly due to meeting the data of surface areas and mass of fuel with affordable mesh sizes, as can be repeatedly found in the literature. For example, the majority of studies on natural smoke control in tunnel fires have been conducted in reduced-scale models with scaling ratios from 1/6 to 1/50 [24]. Numerical validations with full-scale fire tests are scarce as experimental tests represent a high cost and may cause a substantial environmental impact. Four main full-scale fire tests in long tunnels emerge in the literature: the Memorial [25], the Repparfjord [26], the Xianmen [27], and the Norwegian Runehamar [28–30] tunnels.

This work presents the adequateness of a coupled hybrid approach to simulate tunnel ventilation under fire conditions by validating this tool, for the first time, with full-scale data: temperature and velocity profiles. Three Runehamar tunnel fire tests are simulated, with maximum HRR of 6, 66 and 119 MW, being the last two Heavy Good Vehicle (HGV) fire scenarios. A pressure boundary condition to adjust the longitudinal ventilation velocity is suggested when using this approach. Additionally, a critical length expression, previously proposed in Ref. [31], has been assessed with this coupled hybrid methodology, giving satisfactory results. This study validates for the first time the FDS version 6.7.5, which has received important updates in the solver, compared to the versions reported in the literature. Due to this, this work may be more relevant to practitioners who would like to employ the technique presented here, in real-world projects.

The paper firstly presents a brief description of the experimental testing. Afterwards, full CFD and coupled hybrid numerical models for the Runehamar tunnel are defined. Subsequently, numerical results are compared with experimental measurements to validate the coupled hybrid approach as a valuable tool to simulate fire conditions in long tunnels. Finally, the last section is devoted to the conclusions.

2. Case of study: Runehamar tunnel

The Runehamar tunnel is 1600 m long and has a cross-sectional area of 47 m^2 approximately (9 m width and 6 m high). From the east portal, the tunnel presents a slope of 0.5% uphill along the first 500 m, where a plateau is reached and extended 200 m. Then, it follows a 1% downslope of 900 m towards the west portal. Two mobile fan units created the mechanical ventilation of the tunnel. One was located 12 m outside the east tunnel entrance, and the other was inside, about 50–60 m from the portal. Each of them had a volume flow rate of 47.2 m^3/s to guarantee a velocity of 2.4–2.5 m/s after fire ignition, from east to west.

Three fire tests are presented, named Test 0, Test 3 and Test 4. Test 0 consisted of a pool of diesel with a maximum HRR of 6 MW. Test 3 and Test 4 tried to simulate a Heavy Goods Vehicle (HGV) fire with different materials placed on a rack storage system. Test 3 consisted mainly of pieces of furniture, toys and rubber tyres that reached a maximum HRR of 119 MW. Wood pallets, polyester and corrugated paper cartoons were burnt in Test 4, reaching a maximum HRR of 66 MW (Fig. 1 a-c).

In Test 0, the centre of the fire was placed 1037 m from the east portal. The fire sources of Test 3 and Test 4 were moved 2 m upstream and further 5 m, i.e. 1039 and 1042 m, respectively. PROMATECT®-t FIRE protection boards covered the ceiling and the walls around the fire, Fig. 2. The ceiling protection covered a total length of 75 m, from 1015.5 m from the east portal. The walls protection was extended 39 m long, from 1024.5 m from the east portal.

Temperature measurements were obtained at different locations upstream and downstream from the fire source. Further information on the experimental tests can be found in Ref. [29].

3. Materials and methods

The coupled hybrid model is developed with FDS (6.7.5), an open-source CFD software, widely used in the industry, based on Large Eddy Simulations (LES) [32]. The software has a specific HVAC (Heating, Ventilation, and Air Conditioning) sub-model that consists of a network of ducts and nodes. The longer 1D regions of the tunnel, where the flow can be considered uniform, are modelled by these ducts.

The coupling between both domains (3D-CFD and 1D regions) is carried out through HVAC inlet and outlet duct nodes. A single node of the HVAC module is connected to the adjacent cells of the associated vent within the 3D-CFD domain. The interaction between both regions happens in both directions: from the HVAC module to the CFD domain and vice versa. The solution obtained in one of the domains is used as a boundary condition for the solver of the other domain [33].

In the HVAC module, boundary conditions for density, temperature, and pressure are obtained as a weighted average of the adjacent cell values to the vent if the flow enters the duct; or as the mean density and mean temperature for each species, if the flow leaves the duct. Furthermore, volumetric properties, such as the total mass flow and energy, are obtained as the sum of the adjacent cell values.

On the other hand, in the 3D-CFD domain, boundary conditions are established using the properties obtained from the solution of the HVAC module. Moreover, the calculated mass flow rate is considered uniform in all the adjacent cells to the node. Finally, the HVAC solution is uploaded in the predictor and corrector scheme [34]. However, there is a lack of total coupling between FDS and HVAC modules as the pressure solvers are not directly coupled.

The FDS models used to simulate the combustion, turbulence, and radiation are the Eddy Dissipation Concept (EDC) with a thermal extinction model, the Deardorff model ($C_v = 0.1$), and the radiation transport equation with 100 radiation angles, respectively. Furthermore, the maximum number of iterations to solve Poisson equations is increased with respect to the default FDS settings from 10 to 50 (Test 0) and 100 (Test 3 and Test 4) in order to avoid numerical instabilities due to the large size of the 3D-CFD region and the heat release rate influence.

The background velocity of the tunnels is guaranteed by simulating an initial period of 300 s before fire ignition.

3.1. Numerical model of the Runehamar tunnel

The numerical model of the tunnel has a length of 1600 m and a rectangular cross-sectional area of 48 m^2 (8×6 m^2). The Runehamar tunnel has three different slopes (0.5% in the first 500 m, 200 m plateau and −1% in the latter 900 m). As the slope is considered small, and potentially irrelevant in forced ventilation conditions that were present in the experiments, it has made a choice to not model it explicitly. Another important concern in FDS numerical models, with respect to other CFD software, is the lack of definition with irregular geometries. FDS always requires domains with rectilinear volumes. The shape of the ceiling and walls

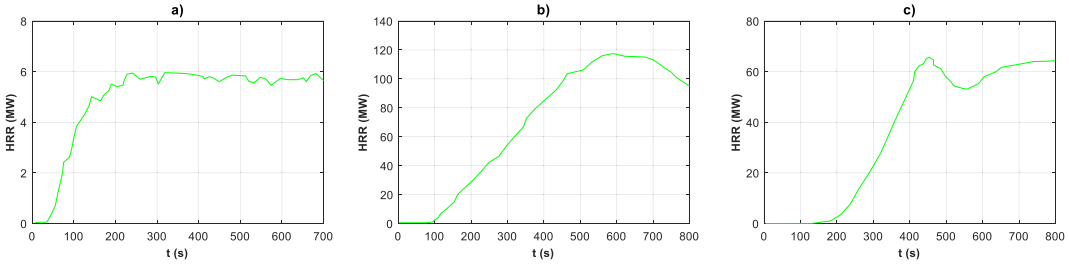

Fig. 1. Heat release rate curves: a) Test 0; b) Test 3; c) Test 4.

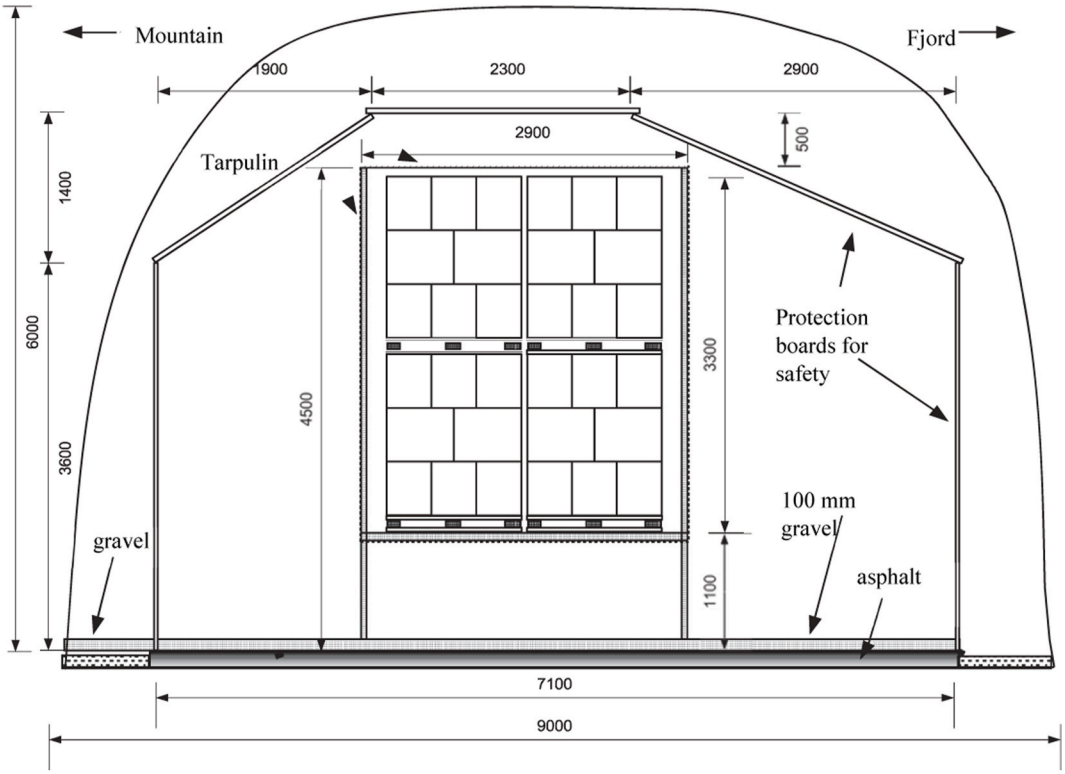

Fig. 2. Tunnel cross-section at the fire site [30].

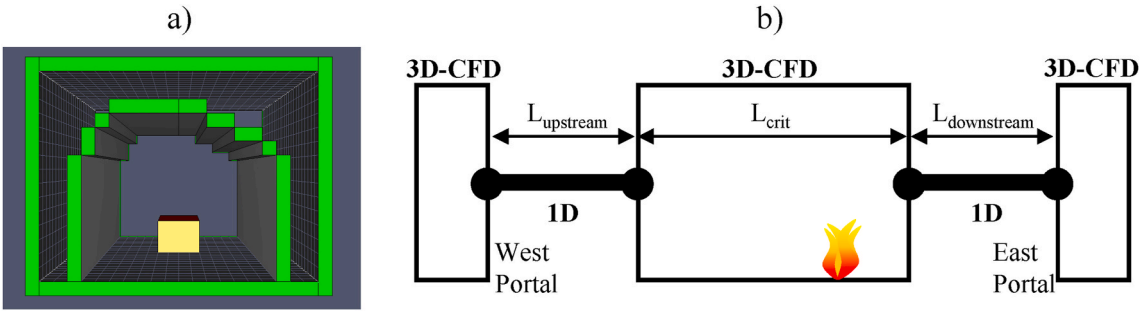

Fig. 3. a) FDS model of the tunnel; b) Scheme of the coupled hybrid model.

protection around the fire source has been approximated, as can be seen in Fig. 3a, for a cell size of 0.4 m, as will be discussed later. They only cover 75 m and 39 m, respectively, from 1024 to 1064 m from the east portal, and are modelled as PROMATEC with a density of 900 kg/m^3, the thermal conductivity of 0.212 W/mK and the specific heat of 1.1 kJ/kg K [29].

Test 0 fire is simulated as a diesel pool fire of 2.4 × 1.6 m^2, which corresponds to the experimental pan with a diameter of 2.2 m, with a radiative fraction of 35%. To search for a simplified and fast model, the porous characteristics of the pallet stack are not considered in Tests 3 and 4. Their fires were simulated with a 3D solid block of 10.4 × 3.2 × 2.8 m^3 (Fig. 3a), which is similar to the dimensions of the HGV trailer mock-up, with a radiative fraction of 45% [35].

Two numerical models are developed: a full 3D model of the tunnel and the coupled hybrid model, with 3D and 1D regions. For the latter, three 3D-CFD and two 1D regions are defined (Fig. 3b). The central 3D-CFD region is extended according to the critical length L_{crit} [31,36], which is obtained by a relationship between the dimensionless critical length L^*_{crit} and heat release rate Q^* :

$$L^*_{crit} = 95(Q^*)^{1/3} \tag{1}$$

where $L^*_{crit} = \frac{L_{crit}}{H}$ and,

$$Q^* = \frac{\dot{Q}}{\rho_\infty C_p T_\infty g^{1/2} \overline{H}^{5/2}} \tag{2}$$

in which $\overline{H}$ is the tunnel hydraulic diameter. This region is considered as a pressure zone as it is a closed part of the domain, [32].

The 1D regions are defined with the same cross-sectional area of the tunnel. There are no reported values of the absolute roughness of the tunnel. A commonly used value of 0.02 m is assumed [19], which corresponds to a friction factor of 0.022, obtained from the Colebrook equation. For every test, the lengths are shown in Table 1.

The 3D-CFD region is not distributed symmetrically to guarantee the backlayering length, being 15–25 m for Test 0 and 100–150 m for Test 3 and Test 4 [29]. To generalize the critical length would require assessing additional fire scenarios. However, this was out of the scope of this work.

The domain is also extended 40 m from both portals to establish atmospheric conditions and to consider possible vena contracta effects, Fig. 3b. This length does not impact on the computational cost of the Full CFD model but it has not been optimized for the coupled hybrid model. The same length has been chosen for both numerical models with the aim to better compare both models. A constant pressure of 45 Pa (Test 0) and 35 Pa (Test 3 and Test 4) was established at the east portal. This value was defined according to the measured flow conditions prior to ignition and remained constant for all the tests. After ignition, the inner fire conditions influenced the centreline velocity, becoming entirely different for every test and changing with time.

A sensitivity analysis with Test 0 is carried out to choose the required mesh resolution by comparing the full-CFD with the experimental results.

3.1.1. Mesh sensitivity analysis

This analysis considers the spatial resolution, $R = D^* / \Delta$, where Δ is the element size and D^* the characteristic diameter of the plume, obtained from the Froude number, calculated as:

$$D^* = \left(\frac{\dot{Q}}{\rho_\infty C_{p,\infty} T_\infty \sqrt{g}} \right)^{2/5} \tag{3}$$

where $\dot{Q}$ is the HRR, ρ_∞ is the air density, $C_{p,\infty}$ is the air specific heat at constant pressure, T_∞ is the air temperature, and g is the gravity acceleration modulus [32].

Five meshes have been tested. Four with a constant element size of 0.2, 0.4, 0.8 and 1.6 m, corresponding to 11.04, 1.38, 0.1825 and 0.023 million cells. The fifth model is defined with an element size of 0.2 m in the near-field, i.e. −37 m and +23 m upstream and downstream from the fire source, and 0.4 m in the rest of the domain. This model has 1.695 million cells. All of them are carried out in a multi-parallel process using 11 cores. The computational cost is directly related to the number of cells to simulate Test 0, reaching 597 h (estimated), 89.7 h, 45.4 h, 4.4 h, 0.47 h, for 0.2, 0.2/0.4, 0.4, 0.8 and 1.6 m cell sizes, respectively. As can be seen, when the cell size is reduced by half (apart from the 0.2/0.4 simulation), the simulation times are multiplied by a factor that ranges from 9 to 13. To compare the results obtained, the time-average temperatures at different downstream locations from the fire source, once the steady-state is reached, i.e. from 400 s to 450 s, are presented in Fig. 4. Three different downstream regions have been analyzed, from 0 to 40 m, from 70 to 200 m, and from 250 to 350 m. It can be observed that 0.2 m, 0.2/0.4 m and 0.4 m cell sizes show similar results in the three regions. The three regions show well-predicted results with discrepancies lower than 18%, 15% and 17%, respectively. However, the results obtained with 0.8 and 1.6 m cell sizes under-predict the temperatures in the three regions with discrepancies up to 39% and 55%. Additionally, the temperature profiles at two distances downstream the fire are also compared in Fig. 5. The 0.2 m, 0.2/0.4 m and 0.4 m cell sizes present similar results with discrepancies lower than 16% between them. Thus, a cell size of 0.4 m guarantees enough precision in both the near and the far fields and is within the resolution range for FDS, $R = 5$, i.e. $5 \leq R \leq 20$. This value is chosen for the coupled hybrid methodology analysis.

Moreover, with this element size, the use of the coupled hybrid methodology leads to a relevant computational saving. The coupled hybrid methodology takes 21.1 h with 6 cores compared with 45.4 h with 11 cores of the full CFD model.

4. Results and discussion

This section presents the numerical results obtained with both the full CFD and coupled hybrid models and their comparison with the full-scale experimental measurements. The temperature profiles at different distances downstream from the fire and the centreline velocity are assessed.

As Fig. 6 shows, the proposed coupled hybrid methodology presents reliable results compared with a full CFD model. For Test 0 (6 MW), both the coupled hybrid and full CFD models predict well the experimental temperatures, particularly when steady-state

Table 1
Lengths of coupled hybrid models.

	1D $L_{upstream}$ [m]	3D-CFD L_{crit} [m]	1D $L_{downstream}$ [m]
Test 0	988	220	392
Test 3	886	592	122
Test 4	886	486	228

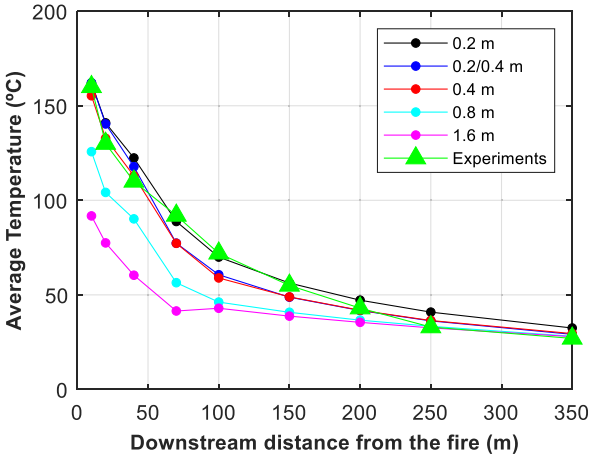

Fig. 4. Time-average temperature at different downstream distances from the fire source in steady-state conditions.

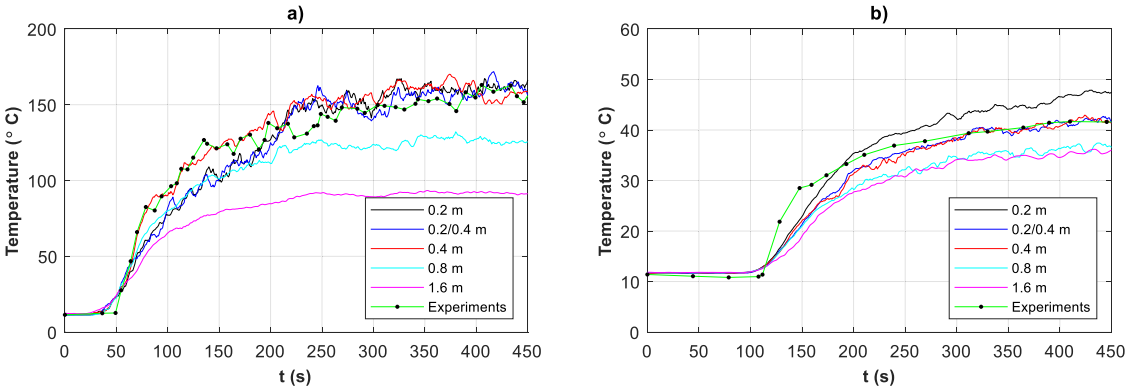

Fig. 5. Temperature profiles at different downstream distances from the fire source: a) 10 m and b) 200 m.

conditions are reached (Fig. 6a), at different locations downstream from the fire, i.e. 10 m, 40 m, 150 m and 200 m. Temperature profiles show the smoke movement downstream of the fire source, reaching a distance of 150 m for the initial 100 s. Gas temperature acts in accordance with the heat release rate curve, Fig. 1a, with a linear growth during the first 200 s. Then after the maximum of 6 MW, the HRR remains nearly constant until the end of the test, which results in the nearly constant behaviour of the temperatures. At location 70 m, the temperature is clearly under-predicted with both numerical models. This might be caused by flow disturbances at this location because of its short distance, only 17 cm, to the extreme of the walls and ceiling protection. Regarding the time-averaged temperature, from 200 s to 700 s after ignition, both numerical models predict the experimental results accurately, with differences lower than 16%, Table 2. In this test, only the velocity at 458 m downstream from the fire source was measured. This location is in the 1D region of the coupled hybrid model, so only the velocity with the full CFD model is compared in Fig. 6b. For the sake of clarity, two positions are compared, i.e. at the heights of 3 m and 4 m. As can be observed, it is slightly under-predicted, which causes the initial delay in the predicted temperatures observed in the farther locations. Moreover, the influence of the fire can be considered negligible on the gas velocity due to the small value of the heat release rate and consequently the small blockage ratio with the tunnel cross-section. In addition, the backlayering length is short, as will be discussed later.

The temperatures in Test 3 (119 MW) are well predicted with both numerical models during the first 600 s of simulation (Fig. 6c). Due to the values so close to the critical velocity, i.e. 2 -3 m/s, the fire grows linearly in this initial period of time, 100–600 s, and the temperature can precisely capture this behaviour. In the experiments, the flame was observed to reach a distance of 70–100 m downstream of the fire, and this is also reproduced by the numerical models. As the peak HRR was achieved, the experimental temperatures started to decrease, being more noticeable at the closest location to the fire source, i.e. 70 m. This cannot be predicted by the numerical models since the fire was simulated by a solid block, and no detailed geometry of the rack storage system was included. During the experiments, the racks collapsed, changing the blockage ratio of the fire and the cross-sectional area of the tunnel. This clearly affects the flow, as can be seen in Fig. 6d. Thus, the central 50 m upstream velocity is under-predicted, decreasing sharply as the HRR grows, approximately 350 s after ignition. Due to the large value of peak HRR, a backlayering length of approximately 100 m upstream of the fire is generated, which consequently also contributes to the reduction of the gas velocity. Also, it has to be mentioned that the experimental evaluation of the HRR included many uncertainties, as described in Ref. [28], estimated as a 14.9%.

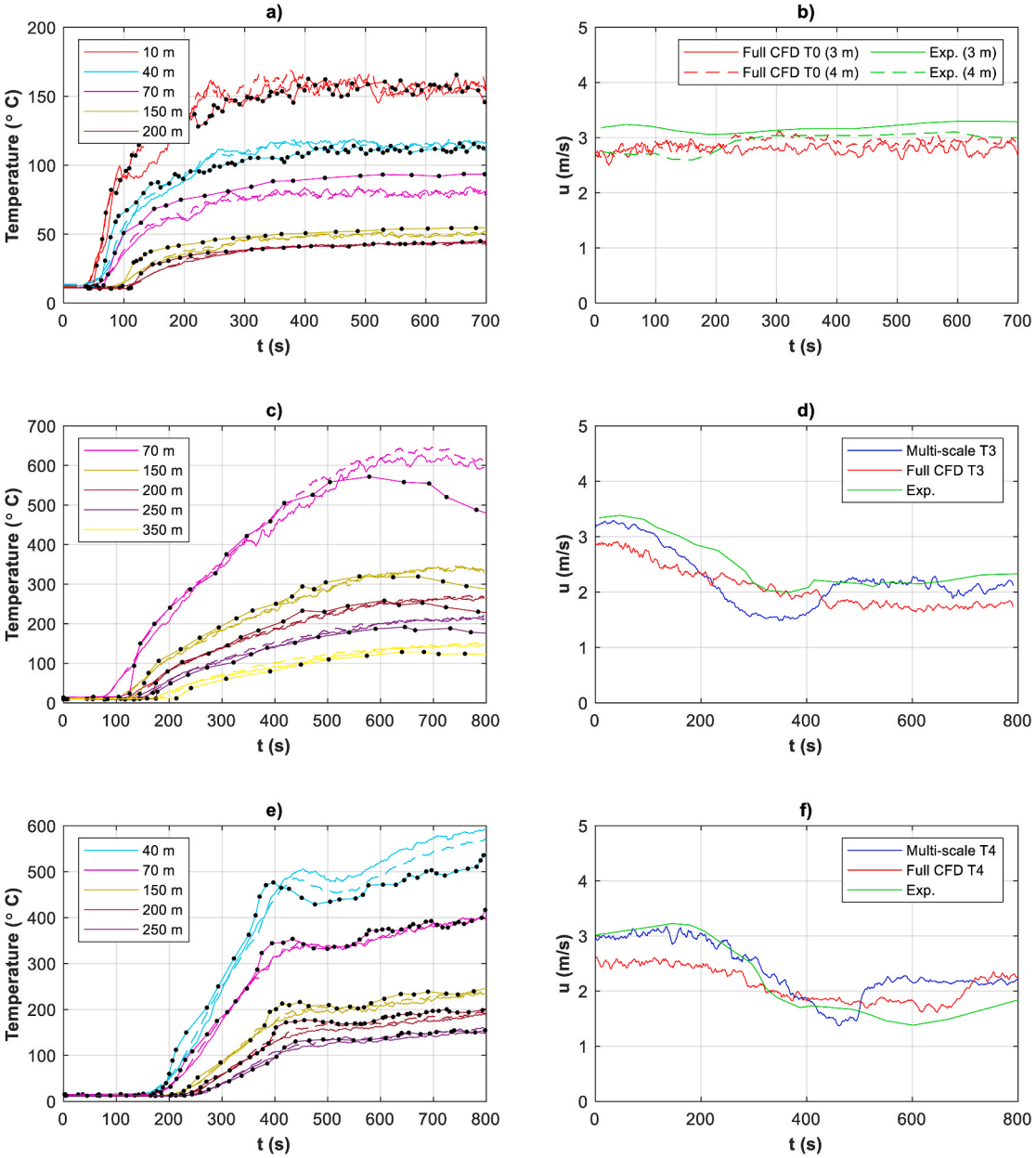

Fig. 6. Temperature profiles at different distances downstream from the fire (Coupled hybrid model: line; Full CFD model: Dash line; Experiments: Dot markers): a) Test 0, c) Test 3, e) Test 4; Central velocity 458 m downstream from the fire: b) Test 0; Central velocity 50 m upstream from the fire: d) Test 3, f) Test 4.

For Test 4 (66 MW), both models present good results in the temperature profiles, Fig. 6e. The gas temperature evolution is similar to the fire curve, Fig. 1c. Due to the initial negligible value of HRR, temperatures remain constant and equal to the ambient temperature during the first 200 s. Then, they start to increase sharply, as the fire grows up until 400 s, when the first peak HRR is achieved. The following variation in the fire behaviour is well captured by the predicted temperatures of both numerical models. As can be observed, the gas temperature follows the same trend as the experimental values. Only at the first location, at 40 m, the temperature is slightly over-predicted. In the same way, the central velocity 50 m upstream from the fire is slightly under-predicted. Nevertheless, gas velocity drops as the fire rises, both numerically and experimentally. It presents a different behaviour after the maximum value of the HRR (Fig. 6f). The following increase in the HRR (Fig. 1c) is not well simulated, mainly because of the definition of a constant fuel surface area. Differences lower than 18% are presented in both numerical models, from 40 m downstream the fire, Table 2.

To quantitively compare the results, Table 2 shows the mean relative and absolute errors in the temperatures of the Full-CFD and coupled hybrid models with respect to the experiments. Test 0 is compared in the steady-state, i.e. from 200 s to 700 s. Test 3 and Test 4 in the initial fire growth period, i.e. from the initial value of 200 s–600 s for Test 3 and to 450 s for Test 4. The three tests are compared

Table 2
Time-averaged absolute and relative ceiling temperature errors at different locations downstream the fire.

Locations (m)			40	70	100	150	200	250
Test 0	[° C]	Full-CFD	5.3	10.5	10.5	3.2	0.7	3.9
		Coupled Hybrid	6.0	9.9	10.0	3.5	1.4	5.2
	[%]	Full-CFD	5	12	15	6	2	12
		Coupled Hybrid	6	11	15	7	3	16
Test 3	[° C]	Full-CFD	119.3	29.5	13.9	7.1	6.6	18.1
		Coupled Hybrid	120.6	17.2	11.6	8.2	8.5	12.4
	[%]	Full-CFD	20	7	4	3	5	17
		Coupled Hybrid	20	4	4	4	5	13
Test 4	[° C]	Full-CFD	21.6	14.0	17.4	15.7	9.0	8.0
		Coupled Hybrid	23.3	15.4	16.7	15.2	8.9	6.7
	[%]	Full-CFD	9	9	18	18	10	15
		Coupled Hybrid	11	9	16	16	10	12

from 40 m to 250 m downstream of the fire. As can be observed, both numerical models present errors in the same order of magnitude at all different positions downstream of the fire. The highest absolute temperature errors achieved depend on the flame influence at the closest locations, particularly as the heat release rate value grows, and reaches 10 m, 70–100 m and 40–70 m, for Test 0, Test 3 and Test 4, respectively. For the coupled hybrid model, due to the small value of the HRR, Test 0 shows a maximum mean difference lower than 10 °C (15%) at 100 m downstream. However, Test 3 presents differences up to 120.6 °C (20%) at 40 m due to the size of the fire but below 11.6 °C (12%) for distances farther than 100 m from the fire source. In the case of Test 4, the maximum differences are also reached at the closest position to the fire, but due to its smaller influence, only a value of 23.3 °C (11%) is reached. The accuracy of the predicted temperatures achieved by the hybrid coupled model confirms this approach as a useful numerical tool to obtain a detailed description of the inner flow of the tunnel with an affordable computational cost.

The maximum ceiling temperature is a key design parameter in tunnel safety, as it directly influences the secureness of tunnel structure. Table 3 presents the maximum ceiling temperatures at different locations upstream and downstream from the fire. In Test 0, the differences between the coupled hybrid and the full CFD models, compared with the experiments, are lower than 18% at locations downstream from the fire. Moreover, the full CFD and coupled hybrid models slightly under-predict the backlayering length, which reaches 5–15 m and corresponds to an error lower than 1% with respect to the total tunnel length. In Test 3, mainly due to the uncertainty in the HRR and the simplified model of the fire, the differences in the temperatures downstream from the fire reach a maximum of 34%. This maximum difference is only for the closest location to the fire (40 m), followed by a maximum value of 19% for the rest of the locations. In Test 4, the differences between the models and experiments are also lower than 19% downstream from the fire. For Test 3 and Test 4, the measured backlayering distances experiments are around 100 m [29]. These distances are much better predicted with the coupled hybrid models. Due to the uncertainties mentioned above, in Test 3, with a very high value of HRR, the backlayering length is under-predicted (40–70 m), which corresponds to an error lower than 4% with respect to the total tunnel length. However, for Test 4, the backlayering length is well predicted, reaching the measured value of 100 m.

Finally, the smoke stratification is studied numerically for the last 100 s of simulation as proposed by Newman [37], who presented a method to differentiate three regions of smoke stratification based on Froude number correlations combined with temperature measurements [37]. Region I, the closest to the fire, is characterized by a clear smoke stratification, whereas region II shows a less severe stratification, and region III no stratification. The criterion is based on the ceiling temperature T_c (at 88% of the tunnel height), the floor temperature T_f (at 12% of the tunnel height), and the average temperature T_{avg} in the cross-section. The dimensionless criterion establishes that Region I (with clear stratification) covers the tunnel length with the ratio of the ceiling and floor temperature difference ($\Delta T_{cf} = T_c - T_f$), and the average temperature and ambient temperature difference ($\Delta T_{avg} = T_{avg} - T_\infty$) higher than 1.7; region II (with less severe stratification) with a ratio lower than 1.7. These ratios are evaluated by their time-averaged values during the last 100 s of simulation, at different locations: 10, 20, 40, 70, 100, 150 and 200 m. As can be seen in Fig. 7, the coupled hybrid methodology and full CFD models are in good agreement with Newmans' criterion. For these locations within the 3D-CFD region, the majority of temperature ratios in both tests are located at Region II, i.e. no clear stratification. Only Test 0 presents some locations on Region I, i.e. clear stratification. This smoke behaviour is explained as the ventilation velocity for cold conditions in both tests is between 2 and 3 m/s, which is close to the critical ventilation velocity and facilitates the smoke dissolution.

5. Conclusions

A complete validation of a coupled hybrid methodology, using an open-source software FDS version 6.7.5 with HVAC, to simulate tunnel ventilation behaviour is assessed for fire conditions. This approach is validated for the first time with full-scale fire tests. Three Runehamar tunnel fire tests are simulated and assessed, with maximum HRR of 6, 66 and 119 MW, being the last two Heavy Good Vehicle (HGV) fire scenarios. A pressure boundary condition to adjust the longitudinal ventilation velocity is proposed, and a critical length expression for the three-dimensional region where the fire is located has been successfully assessed.

The adequateness of the approach to simulate tunnel fire incidents is proved by comparing the gas temperature below the ceiling at

Table 3
Maximum gas temperature (°C) at different locations.

Locations [m]		−100	−70	−40	−25	−15	0	10	40	70	100	150	200	250
0	Experiments	11	11	11	11	144	267	166	114	94	74	55	45	36
	Coupled hybrid	–	–	–	11	11	188	174	119	86	63	52	46	–
	Full CFD	11	11	11	11	21	183	169	112	77	57	43	37	32
3	Experiments	72	121	187	285	462	1281	1195	740	572	421	335	261	193
	Coupled hybrid	12	12	59	72	286	1239	1322	995	698	511	368	286	229
	Full CFD	11	11	11	18	221	1177	1407	991	680	479	350	271	215
4	Experiments	43	87	149	214	448	1305	*	556	426	329	266	214	170
	Coupled hybrid	53	76	101	136	394	1211	974	661	457	357	272	220	179
	Full CFD	11	11	42	59	305	1137	862	536	385	305	231	186	154

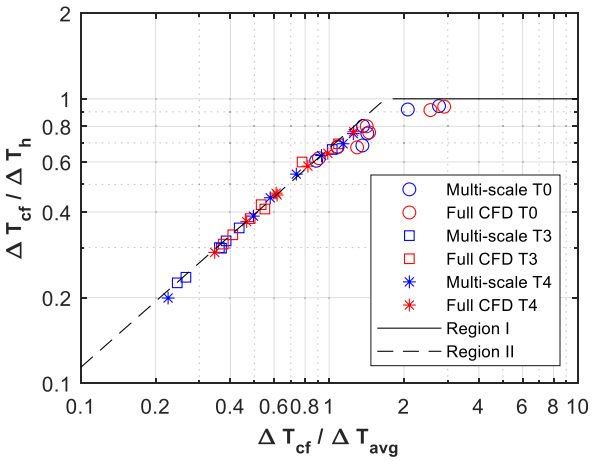

Fig. 7. Temperature stratification in Newman's temperature diagram [37].

various locations upstream and downstream the fire, and the centreline velocity. The predictions of the time-averaged temperature reach errors lower than 20% with respect to the experimental measurements in the downstream region, beyond 40 m from the fire source. Furthermore, under the circumstances studied, the coupled hybrid methodology predicts well the backlayering length with errors lower than 4% compared to the total tunnel length. The maximum temperature differences between the models and the experiments are lower than 19%, farther than 70 m downstream the fire, and slightly enlarged up to 34% at 40 m for the largest fire.

In summary, this coupled hybrid methodology presents reliable results in tunnel ventilation systems when modelling fire conditions with a restrained computational cost. Time savings between 27% and 75% with respect to a full-CFD numerical have been achieved. The numerical results confirm that the proposed coupled hybrid approach presents accurate predictions of the temperature fields. Additional important fire safety factors such as maximum temperatures, centreline velocities, and backlayering distances are also well predicted. This work may be relevant to practitioners who would like to employ the technique presented here, in real-world projects.

Author statement

Diego Álvarez-Coedo (First Author): Conceptualization, Methodology, Software, Investigation, Formal Analysis, Writing - Original Draft, Funding acquisition; **Pablo Ayala (Corresponding Author):** Conceptualization, Methodology, Software, Investigation, Formal analysis, Writing - Original Draft; **Alexis Cantizano:** Conceptualization, Formal analysis, Investigation, Writing - Review & Editing, Funding acquisition; **Wojciech Wegrzynski:** Conceptualization, Validation, Investigation, Writing - Review & Editing, Funding acquisition.

Declaration of competing interest

The authors declare that they have no known competing financial interests or personal relationships that could have appeared to influence the work reported in this paper.

Acknowledgements

The authors want to acknowledge the Society of Fire Protection Engineer (SFPE) Foundation for supporting this research with a Student Research Grants and the National Institute of Standard and Technology for making FDS available. Thank you to the Institute for Research in Technology (IIT) of Comillas Pontifical University and the Instytut Techniki Budowlanej (ITB) for their support.

References

[1] R. Carvel, A review of tunnel fire research from Edinburgh, Fire Saf. J. 105 (abril de 2019) 300–306, https://doi.org/10.1016/j.firesaf.2016.02.004. Elsevier Ltd.

[2] R.K. Haddad, R. Zulkifli, C. Maluk, y Z. Harun, Experimental investigation on the influences of different horizontal fire locations on smoke temperature stratification under tunnel ceiling, J. Appl. Fluid Mech. 13 (4) (2020) 1289–1298, https://doi.org/10.36884/JAFM.13.04.30876.

[3] J. Kong, Z. Xu, W. You, B. Wang, Y. Liang, y T. Chen, Study of smoke back-layering length with different longitudinal fire locations in inclined tunnels under natural ventilation, Tunn. Undergr. Space Technol. 107 (ene. 2021), 103663, https://doi.org/10.1016/j.tust.2020.103663.

[4] X. Yang, Y. Luo, Z. Li, H. Guo, y Y. Zhang, Experimental investigation on the smoke back-layering length in a branched tunnel fire considering different longitudinal ventilations and fire locations, Case Stud. Therm. Eng. 28 (dic. 2021), 101497, https://doi.org/10.1016/j.csite.2021.101497.

[5] L. Yi, et al., Flow field and fire characteristics inside a tunnel under the influence of canyon cross wind, Tunn. Undergr. Space Technol. 105 (nov. 2020), 103575, https://doi.org/10.1016/j.tust.2020.103575.

[6] A. Król y, M. Król, Numerical investigation on fire accident and evacuation in a urban tunnel for different traffic conditions, Tunn. Undergr. Space Technol. 109 (mar. 2021), 103751, https://doi.org/10.1016/j.tust.2020.103751.

[7] J. Luo, Z. Xu, F. Li, y J. Zhao, Effect of vehicular blocking scene on smoke spread in the longitudinal ventilated tunnel fire, Case Stud. Therm. Eng. 14 (sep. 2019), 100495, https://doi.org/10.1016/j.csite.2019.100495.

[8] R. Pan, et al., Experimental investigation of maximum temperature and longitudinal temperature distribution induced by linear fire in portals-sealed tunnel, Case Stud. Therm. Eng. 23 (feb. 2021), 100804, https://doi.org/10.1016/j.csite.2020.100804.

[9] Y. Yao, K. He, M. Peng, L. Shi, X. Cheng, y H. Zhang, Maximum gas temperature rise beneath the ceiling in a portals-sealed tunnel fire, Tunn. Undergr. Space Technol. 80 (oct. 2018) 10–15, https://doi.org/10.1016/j.tust.2018.05.021.

[10] M. Weng, I. Obadi, F. Wang, F. Liu, y C. Liao, Optimal distance between jet fans used to extinguish metropolitan tunnel fires: a case study using fire dynamic simulator modeling, Tunn. Undergr. Space Technol. 95 (2020), 103116, https://doi.org/10.1016/j.tust.2019.103116.

[11] W. Wang, Z. Zhu, Z. Jiao, H. Mi, y Q. Wang, Characteristics of fire and smoke in the natural gas cabin of urban underground utility tunnels based on CFD simulations, Tunn. Undergr. Space Technol. 109 (mar. 2021), 103748, https://doi.org/10.1016/j.tust.2020.103748.

[12] M. Shirzadi, P.A. Mirzaei, y Y. Tominaga, CFD analysis of cross-ventilation flow in a group of generic buildings: comparison between steady RANS, LES and wind tunnel experiments, Build. Simulat. 13 (6) (jul. 2020) 1353–1372, https://doi.org/10.1007/S12273-020-0657-7, 2020 13:6.

[13] B. Ralph y, R. Carvel, Coupled hybrid modelling in fire safety engineering; a literature review, Fire Saf. J. 100 (septiembre de 2018) 157–170, https://doi.org/10.1016/j.firesaf.2018.08.008. Elsevier Ltd.

[14] F. Colella, G. Rein, R. Borchiellini, y J.L. Torero, A novel multiscale methodology for simulating tunnel ventilation flows during fires, Fire Technol. 47 (1) (2011) 221–253.

[15] M. Pachera, X. Deckers, y T. Beji, Capabilities and limitations of the fire dynamics simulator in the simulation of tunnel fires with a multiscale Approach, J. Phys.: Conf. Ser. 1107 (nov. 2018), 042016, https://doi.org/10.1088/1742-6596/1107/4/042016.

[16] C. Xu, Y. Li, X. Feng, y J. Li, Multi-scale coupling analysis of partial transverse ventilation system in an underground road tunnel, Procedia Eng. 211 (ene. 2018) 837–843, https://doi.org/10.1016/j.proeng.2017.12.082.

[17] F. Colella, G. Rein, R. Borchiellini, R. Carvel, J.L. Torero, y V. Verda, Calculation and design of tunnel ventilation systems using a two-scale modelling approach, Build. Environ. 44 (12) (2009) 2357–2367, https://doi.org/10.1016/j.buildenv.2009.03.020.

[18] F. Colella, G. Rein, R. Carvel, P. Reszka, y J.L. Torero, Analysis of the ventilation systems in the Dartford tunnels using a multi-scale modelling approach, Tunn. Undergr. Space Technol. 25 (4) (jul. 2010) 423–432, https://doi.org/10.1016/j.tust.2010.02.007.

[19] C.D.E. Ang, G. Rein, J. Peiro, y R. Harrison, Simulating longitudinal ventilation flows in long tunnels: comparison of full CFD and multi-scale modelling approaches in FDS6, Tunn. Undergr. Space Technol. 52 (feb. 2016) 119–126, https://doi.org/10.1016/j.tust.2015.11.003.

[20] I. Vermesi, G. Rein, F. Colella, M. Valkvist, y G. Jomaas, Reducing the computational requirements for simulating tunnel fires by combining multiscale modelling and multiple processor calculation, Tunn. Undergr. Space Technol. 64 (2017) 146–153, https://doi.org/10.1016/j.tust.2016.12.016.

[21] C.D. Ang, G. Rein, y J. Peiro, Unexpected oscillations in fire modelling inside a long tunnel, Fire Technol. (jun. 2020) 1–5, https://doi.org/10.1007/s10694-020-01004-x.

[22] K. McGrattan y, R. McDermott, Response to “Unexpected Oscillations in Fire Modelling Inside a Long Tunnel” by Ang et al, Fire Technol. (ago. 2021) 1–5, https://doi.org/10.1007/S10694-021-01166-2, 2021.

[23] M.S. Tomar y, S. Khurana, Investigation of road tunnel fires: challenges and findings, J. Phys.: Conf. Ser. 1276 (1) (ago. 2019), 012065, https://doi.org/10.1088/1742-6596/1276/1/012065.

[24] P. Lin, Y.-Y. Xiong, C. Zuo, y J.-K. Shi, Verification of similarity of scaling laws in tunnel fires with natural ventilation, Fire Technol. 57 (4) (jul. 2021) 1611–1635, https://doi.org/10.1007/s10694-020-01084-9.

[25] Massachusetts Highway Department, Memorial Tunnel Fire Ventilation Test Program, 1996.

[26] A. Haack, Fire protection in traffic tunnels: general aspects and results of the EUREKA project, Tunn. Undergr. Space Technol. 13 (4) (oct. 1998) 377–381, https://doi.org/10.1016/S0886-7798(98)00080-7.

[27] T. Yan, S. MingHeng, G. YanFeng, y H. JiaPeng, Full-scale experimental study on smoke flow in natural ventilation road tunnel fires with shafts, Tunn. Undergr. Space Technol. 24 (6) (nov. 2009) 627–633, https://doi.org/10.1016/j.tust.2009.06.001.

[28] A. Lönnermark y, H. Ingason, Gas temperatures in heavy goods vehicle fires in tunnels, Fire Saf. J. 40 (6) (sep. 2005) 506–527, https://doi.org/10.1016/j.firesaf.2005.05.003.

[29] H. Ingason, A. Lönnermark, y Y.Z. Li, Runehamar tunnel Fire tests», 2011.

[30] H. Ingason, Y.Z. Li, y A. Lönnermark, Runehamar tunnel fire tests, Fire Saf. J. 71 (2015) 134–149, https://doi.org/10.1016/j.firesaf.2014.11.015.

[31] Z. Wang, X. Jiang, F. Tang, y J. Li, Study on critical length for simulation in tunnel fires, Tunn. Undergr. Space Technol. 115 (sep. 2021), 104013, https://doi.org/10.1016/J.TUST.2021.104013.

[32] K. McGrattan, R. McDermott, S. Hostikka, y J. Floyd, «FDS (Version 6) User’s Guide, Technical report, NIST, 2013.

[33] J. Floyd, Coupling a network HVAC model to a computational fluid dynamics model using large eddy simulation, Fire Saf. Sci. 10 (2011) 459–470.

[34] K.B. McGrattan, S. Hostikka, J.E. Floyd, W.E. Mell, y R. McDermott, Fire Dynamics Simulator, Technical Reference Guide, Volume 1: Mathematical Model, vol. 1018, NIST Special Publication, 2013.

[35] Y.Z. Li, H. Ingason, y A. Lönnermark, Numerical simulation of Runehamar tunnel fire tests, in: 6th International Conference Tunnel Safety and Ventilation, 2012, pp. 203–210.

[36] Z. Wang, X. Jiang, H. Park, L. Wang, y J. Wang, Numerical Investigation on the length of the near-field region of smoke flow in tunnel fires, Case Stud. Therm. Eng. 28 (dic. 2021), 101584, https://doi.org/10.1016/j.csite.2021.101584.

[37] J.S. Newman, Experimental evaluation of fire-induced stratification, Combust. Flame 57 (1) (jul. 1984) 33–39, https://doi.org/10.1016/0010-2180(84)90135-4.